

Rafał BROCIEK, Damian SŁOTA

Institute of Mathematics, Silesian University of Technology, Gliwice, Poland

IMPLICIT FINITE DIFFERENCE METHOD FOR THE SPACE FRACTIONAL HEAT CONDUCTION EQUATION WITH THE MIXED BOUNDARY CONDITION

Abstract. This paper presents the numerical solution of the space fractional heat conduction equation with Neumann and Robin boundary conditions. In described equation the Riemann-Liouville fractional derivative is used. Considered model is solved by using the implicit finite difference method. The paper also presents the numerical examples to illustrate the accuracy and stability of described method.

1. Introduction

In recent years the fractional derivatives became very popular in modeling various types of phenomena occurring in biology, physics, engineering, as well as in the control theory [2, 7, 15, 17, 19]. Often, we are not able to solve these models in an analytical way, therefore it is important to develop the approximate methods dedicated for solving the fractional differential equations.

Murio in his paper [16] presents the solution of the time fractional diffusion equation with zero boundary condition by using the implicit finite difference method. He applies in his work the Caputo fractional derivative. In paper [1],

2010 Mathematics Subject Classification: 35R11, 35K05, 65M06.

Keywords: space fractional heat conduction equation, implicit finite difference method.

Corresponding author: R. Brociek (Rafal.Brociek@polsl.pl).

Received: 21.06.2016.

the author considers the time fractional heat conduction equation with Neumann and Robin boundary conditions and the Caputo fractional derivative. To solve this equation, the implicit finite difference scheme is used. Next, in work [20] the authors present the numerical scheme for fractional heat equation with Dirichlet and Neumann boundary conditions.

In paper [3] the authors describe the numerical method for the fractional diffusion equation with Dirichlet boundary conditions. In this approach the finite difference method and the Kansa method are used to solve the considered equation. While paper [8] presents the numerical solution of the differential equation with fractional derivative with respect to the spatial variable. The fractional derivative applied to this model is the Riemann-Liouville fractional derivative and the authors use the finite volume method.

In paper [21] authors consider the space fractional diffusion equation with Dirichlet boundary conditions and the Caputo derivative. To solve this equation the authors use the Chebyshev polynomials of the third kind. Paper [5] presents the numerical solution of the fractional diffusion equation with Dirichlet boundary conditions. The authors use in this elaboration the Crank-Nicolson scheme to solve the equation and then they prove the stability and convergence of the proposed method. Another publication in which we can find some information about the fractional differential equations and their numerical solution is [6].

Also Meerschaert and Tadjeran deal with the numerical methods of solving the differential equations with fractional derivative [10–12, 22]. Paper [22] shows the numerical solution of the fractional diffusion equation with fractional derivative with respect to the spatial variable and with the first kind boundary conditions, while in work [10] the authors investigate the numerical solution of the two-dimensional fractional dispersion equation. In both papers the fractional derivative is taken with respect to the spatial variable and it is expressed as the Riemann-Liouville fractional derivative.

In this paper, the space fractional heat conduction equation is considered and its numerical solution is found. The investigated equation is completed by the Neumann and Robin boundary conditions and as the fractional derivative the authors apply the Riemann-Liouville derivative. In order to solve the described model, the implicit finite difference scheme is used and $O(h^2)$ approximations for the boundary conditions is applied. The paper includes also the examples to illustrate the accuracy and stability of described method.

2. Formulation of the problem

Let us consider the following heat conduction equation with fractional derivative with respect to the spatial variable

$$c\rho \frac{\partial u(x,t)}{\partial t} = -v(x) \frac{\partial u(x,t)}{\partial x} + \lambda(x) \frac{\partial^\alpha u(x,t)}{\partial x^\alpha} + g(x,t), \quad (1)$$

defined in region $D = \{(x,t) : x \in [a,b], t \in [0,T]\}$. In this work, we use the terminology adopted for the case of classical heat conduction equation, despite of the change of some units, so λ denotes here the thermal conductivity coefficient, c and ρ are the specific heat and the density, respectively. We assume that $v(x) \geq 0$, $\lambda(x) > 0$ for $x \in [a,b]$. For equation (1) there are posed the initial condition

$$u(x,0) = f(x), \quad x \in [a,b], \quad (2)$$

and the boundary conditions of the second and third kind

$$-\lambda(a) \frac{\partial u(a,t)}{\partial x} = q(t), \quad t \in [0,T], \quad (3)$$

$$-\lambda(b) \frac{\partial u(b,t)}{\partial x} = h(t)(u(b,t) - u^\infty), \quad t \in [0,T], \quad (4)$$

where h is the heat transfer coefficient, q means the heat flux and u^∞ denotes the ambient temperature.

Fractional derivative occurring in the described model is expressed as the Riemann-Liouville fractional derivative defined by [17]:

$$\frac{\partial^\alpha u(x,t)}{\partial x^\alpha} = \frac{1}{\Gamma(n-\alpha)} \frac{\partial^n}{\partial x^n} \int_a^x u(s,t)(x-s)^{n-1-\alpha} ds, \quad (5)$$

where $\alpha \in (n-1, n]$ and $\Gamma(\cdot)$ is the Gamma function [18]. In case of $\alpha \in (1, 2)$, equation (1) describes the super-diffusion phenomenon [9, 13], and for $\alpha = 2$ we obtain the model with classical derivative.

3. Numerical solution

In this section, we describe the numerical solution of model (1)-(4) determined by using the finite difference method. Let $N, M \in \mathbb{N}$ are the sizes of grid for the

spatial and time variable, respectively. We set the grid steps $\Delta x = \frac{(b-a)}{N}$ and $\Delta t = T/M$. Thus we get the following grid

$$S = \{(x_i, t_k) : x_i = a + i \Delta x, t_k = k \Delta t, i = 0, 1, \dots, N, k = 0, 1, 2, \dots, M\}. \quad (6)$$

We assume the following notation $\lambda_i = \lambda(x_i)$, $v_i = v(x_i)$, $g_i^k = g(x_i, t_k)$, $f_i = f(x_i)$, $h^k = h(t_k)$. The values of approximate function in points (x_i, t_k) are denoted by U_i^k ($U_i^k \approx u(x_i, t_k)$).

In order to approximate the fractional derivative (5), we use the Grünwald formula [14]:

$$\frac{\partial^\alpha u(x, t)}{\partial x^\alpha} = \frac{1}{\Gamma(-\alpha)} \lim_{\bar{N} \rightarrow \infty} \frac{1}{r^\alpha} \sum_{j=0}^{\bar{N}} \frac{\Gamma(j-\alpha)}{\Gamma(j+1)} u(x - (j-1)r, t), \quad (7)$$

where $r = \frac{x-a}{\bar{N}}$. We also assume the notation

$$\omega_{\alpha, j} = \frac{\Gamma(j-\alpha)}{\Gamma(-\alpha)\Gamma(j+1)}. \quad (8)$$

The discrete form of equation (1) is presented as follows ($i = 1, 2, \dots, N-1$):

$$\frac{U_i^{k+1} - U_i^k}{\Delta t} = -v_i \frac{U_i^{k+1} - U_{i-1}^{k+1}}{c\varrho\Delta x} + \frac{\lambda_i}{c\varrho(\Delta x)^\alpha} \sum_{j=0}^{i+1} \omega_{\alpha, j} U_{i-j+1}^{k+1} + \frac{g_i^{k+1}}{c\varrho}. \quad (9)$$

Rearranging equation (9), we obtain ($i = 1, 2, \dots, N-1$):

$$\begin{aligned} -\omega_{\alpha, 0} \frac{\lambda_i \Delta t}{c\varrho(\Delta x)^\alpha} U_{i+1}^{k+1} + \left(1 + \frac{v_i \Delta t}{c\varrho\Delta x} - \omega_{\alpha, 1} \frac{\lambda_i \Delta t}{c\varrho(\Delta x)^\alpha}\right) U_i^{k+1} - \\ - \left(\frac{v_i \Delta t}{c\varrho\Delta x} + \omega_{\alpha, 2} \frac{\lambda_i \Delta t}{c\varrho(\Delta x)^\alpha}\right) U_{i-1}^{k+1} - \frac{\lambda_i \Delta t}{c\varrho(\Delta x)^\alpha} \sum_{j=3}^{i+1} \omega_{\alpha, k} U_{i-j+1}^{k+1} = \\ = U_i^k + \frac{\Delta t g_i^{k+1}}{c\varrho}. \end{aligned} \quad (10)$$

The Neumann boundary condition is approximated as follows

$$-\lambda_0 \left(\frac{-U_2^{k+1} + 4U_1^{k+1} - 3U_0^{k+1}}{2\Delta x} \right) = q^{k+1}, \quad (11)$$

and the Robin boundary condition is approximated in the form

$$-\lambda_N \left(\frac{U_{N-2}^{k+1} - 4U_{N-1}^{k+1} + 3U_N^{k+1}}{2\Delta x} \right) = h^{k+1}(U_N^{k+1} - u^\infty). \tag{12}$$

By using the approximations of boundary conditions, equation (10) may be rewritten in the matrix form

$$\mathbf{A}\bar{U}^{k+1} = \bar{U}^k + \bar{G}^{k+1} \Delta t, \quad k = 0, 1, 2, \dots, \tag{13}$$

where

$$\begin{aligned} \bar{U}^k &= [U_0^k, U_1^k, \dots, U_N^k]^T, \\ \bar{G}^{k+1} \Delta t &= \left[q^{k+1}, \frac{g_1^{k+1} \Delta t}{c\rho}, \frac{g_2^{k+1} \Delta t}{c\rho}, \dots, \frac{g_{N-1}^{k+1} \Delta t}{c\rho}, -h^{k+1}u^\infty \right], \end{aligned}$$

matrix \mathbf{A} is of size $(N + 1) \times (N + 1)$ and we have the following coefficients:

$$a_{ij} = \begin{cases} \frac{3\lambda_0}{2\Delta x}, & j = i = 0, \\ \frac{-2\lambda_0}{\Delta x}, & j = 1 \wedge i = 0, \\ \frac{\lambda_0}{2\Delta x}, & j = 2 \wedge i = 0, \\ -\frac{v_i \Delta t}{c\rho \Delta x} - \omega_{\alpha,2} \frac{\lambda_i \Delta t}{c\rho(\Delta x)^\alpha}, & j = i - 1 \wedge i \neq 0 \wedge i \neq N, \\ 1 + \frac{v_i \Delta t}{c\rho \Delta x} - \omega_{\alpha,1} \frac{\lambda_i \Delta t}{c\rho(\Delta x)^\alpha}, & j = i \wedge i \neq N \wedge i \neq 0, \\ -\omega_{\alpha,0} \frac{\lambda_i \Delta t}{c\rho(\Delta x)^\alpha}, & j = i + 1 \wedge i \neq 0 \wedge i \neq N, \\ -\omega_{\alpha,i-j+1} \frac{\lambda_i \Delta t}{c\rho(\Delta x)^\alpha}, & j \leq i - 2, \\ 0 & j \geq i + 2, \\ -\frac{\lambda_N}{2\Delta x} & j = N - 2 \wedge i = N, \\ \frac{2\lambda_N}{\Delta x} & j = N - 1 \wedge i = N, \\ -\frac{3\lambda_N}{2\Delta x} - h^{k+1} & j = i = N. \end{cases}$$

On the way of solving the system of equations defined by (13), we obtain the approximate values of function u in the grid points (6).

In paper [22], we can find the proof of unconditional stability of the presented method in case of the homogeneous Dirichlet and Neumann boundary conditions defined, respectively, on the left and the right end of the considered interval. By conducting the similar reasoning, it can be proven that the method discussed in this paper is unconditionally stable for the considered boundary conditions.

4. Numerical examples

In this section we show some examples to illustrate the accuracy of presented method.

Example 1. Let us consider equation (1) defined in region

$$D = \{(x, t) : x \in [0, 1], t \in [0, 1]\},$$

with the following data

$$\alpha = 1.8, \quad \lambda(x) = \frac{1}{6}\Gamma(2.2)x^{2.8}, \quad c = \varrho = 1, \quad u^\infty = 50,$$

$$g(x, t) = -(1+x)x^3e^{-t}, \quad h(t) = -\frac{0.550901e^{-t}}{e^{-t} - 50}, \quad v(x) = 0, \quad q(t) = 0.$$

The initial condition has the form

$$u(x, 0) = x^3, \quad x \in (0, 1).$$

The exact solution of considered problem is of the following form

$$u(x, t) = x^3e^{-t}.$$

Let us define now the maximal and average errors of the approximate solution

$$\Delta_{\max} = \max_{\substack{0 \leq i \leq N \\ 1 \leq k \leq M}} |u_i^k - U_i^k|,$$

$$\Delta_{\text{avg}} = \frac{1}{(N+1)(M+1)} \sum_{i=0}^N \sum_{k=0}^M |u_i^k - U_i^k|.$$

Table 1 includes the errors of approximate solution for the different grids. As we can see, with the increase of second dimension M of the grid, for the first dimension N fixed, the errors decrease. For example, where $N = 100$ and $M = 100, 200, 300$, the absolute errors do not exceed $1.95 \cdot 10^{-3}$, $1.16 \cdot 10^{-3}$ and $8.92 \cdot 10^{-4}$, respectively. Increasing the dimension of grid with respect to the spatial variable, for the dimension M fixed, we observe a slight decrease of the approximate solution errors.

Table 1
 Maximal errors Δ_{\max} and average errors Δ_{avg}
 calculated for the respective grids (example 1)

Grid $N \times M$	Δ_{\max}	Δ_{avg}
10×10	$1.7162 \cdot 10^{-2}$	$4.6937 \cdot 10^{-3}$
10×30	$7.2131 \cdot 10^{-3}$	$2.0595 \cdot 10^{-3}$
20×20	$9.1951 \cdot 10^{-3}$	$2.4490 \cdot 10^{-3}$
50×50	$3.8367 \cdot 10^{-3}$	$1.0033 \cdot 10^{-3}$
100×100	$1.9459 \cdot 10^{-3}$	$5.0549 \cdot 10^{-4}$
100×200	$1.1558 \cdot 10^{-3}$	$3.0121 \cdot 10^{-4}$
100×300	$8.9191 \cdot 10^{-4}$	$2.3289 \cdot 10^{-4}$
200×100	$1.7713 \cdot 10^{-3}$	$4.5775 \cdot 10^{-4}$
300×100	$1.7110 \cdot 10^{-3}$	$4.4155 \cdot 10^{-4}$

In Figure 1, we can see the distribution of errors in the grid points. The largest errors occur at the final moment of time $t = 1$ and for $x = 1$. Figure 2 presents the exact solution, the approximate solution and the errors in time $t = 1$. The approximate solution fits very well to the exact solution, the largest error occurs in point $x = 1$ and does not exceed 0.002.

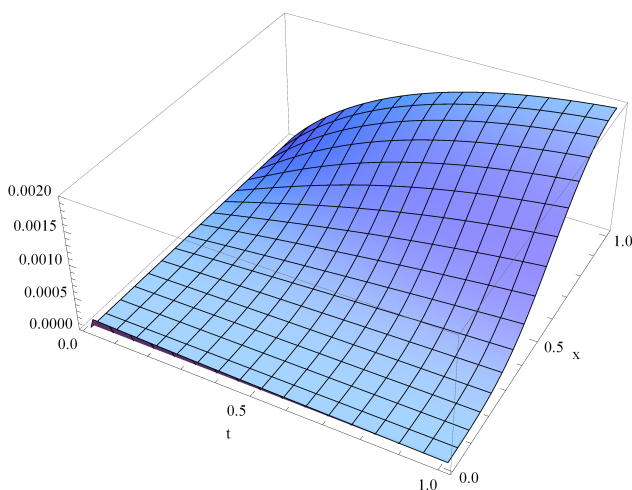


Fig. 1. Distribution of errors of approximate solution ($N = M = 100$) (example 1)

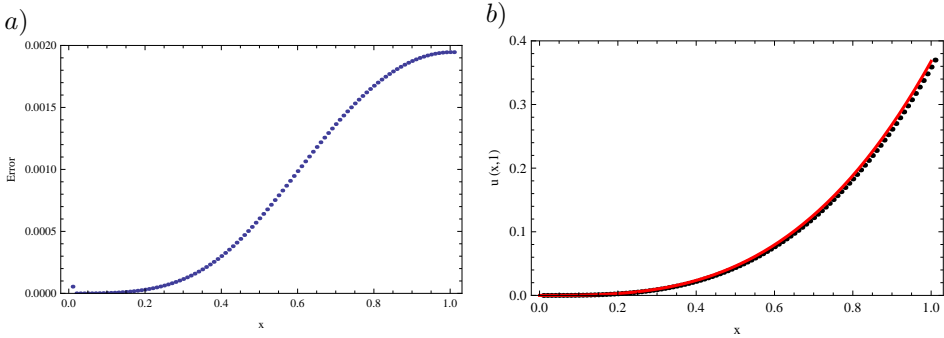


Fig. 2. Distribution of errors (a) together with the approximate solution (dots) and the exact solution (solid line) (b) in time $t = 1$ ($N = M = 100$) (example 1)

Example 2. Again, we consider equation (1) but this time with the following data

$$\alpha = 1.9, \quad \lambda(x) = \frac{1}{2}, \quad c = \varrho = 1, \quad u^\infty = 100, \quad a = 1, \quad b = 2,$$

$$g(x, t) = -2t(x - 1) + 0.0525569(t^2 - 1) \left(\frac{32.7273 - 32.7273x}{(x - 1)^{1.9}} + \frac{18.1818}{(x - 1)^{0.9}} + \frac{15.5455 - 31.0909x + 15.5455x^2}{(x - 1)^{2.9}} \right),$$

$$h(t) = \frac{(1 - t^2)}{2(99 + t^2)}, \quad v(x) = 0, \quad q(t) = \frac{1}{2}(t^2 - 1).$$

The problem is completed by the initial condition

$$u(x, 0) = x - 1, \quad t \in [0, 1].$$

The exact solution for this example is given by the following function

$$u(x, t) = (x - 1)(1 - t^2).$$

Table 2 presents the errors of approximate solution for the different grids. Similar as in example 1, by decreasing step Δt of the grid we cause the significant decrease of errors Δ_{avg} and Δ_{max} of the approximate solution. Moreover, increase of the grid density with respect to the spatial variable results in a slight decrease of errors.

Table 2
 Maximal errors Δ_{\max} and average errors Δ_{avg}
 calculated for the respective grids (example 2)

Grid $N \times M$	Δ_{\max}	Δ_{avg}
10×10	$5.8912 \cdot 10^{-2}$	$2.4749 \cdot 10^{-2}$
10×50	$1.3121 \cdot 10^{-2}$	$6.0376 \cdot 10^{-3}$
20×20	$2.9118 \cdot 10^{-2}$	$1.2127 \cdot 10^{-2}$
50×50	$1.1462 \cdot 10^{-2}$	$4.7135 \cdot 10^{-3}$
100×100	$5.6665 \cdot 10^{-3}$	$2.3089 \cdot 10^{-3}$
100×200	$2.9806 \cdot 10^{-3}$	$1.2908 \cdot 10^{-3}$
100×300	$2.0838 \cdot 10^{-3}$	$9.5044 \cdot 10^{-4}$
200×100	$5.4641 \cdot 10^{-3}$	$2.1286 \cdot 10^{-3}$
300×100	$5.3918 \cdot 10^{-3}$	$2.0635 \cdot 10^{-3}$

Distribution of errors in domain D for Example 2 is presented in Figure 3. The largest error, about 0.005, is observed in time $t = 1$ and for $x = 1$. On the left boundary of variable x the errors are smaller than on the right boundary. We also present the errors of approximate solution in time $t = 1$ (see Figure 4). The absolute error is smaller than 0.006 and the largest error is observed for $x = 2$.

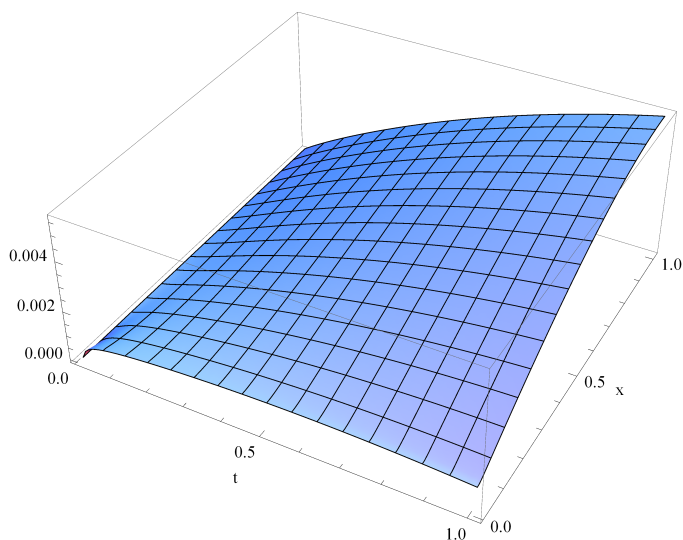


Fig. 3. Distribution of errors of approximate solution ($N = M = 100$) (example 2)

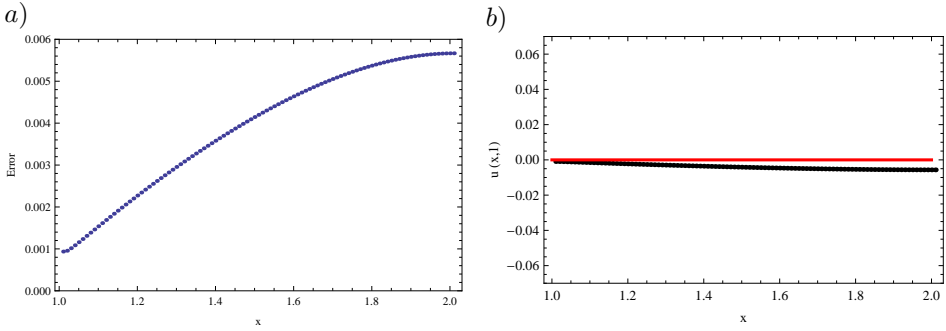


Fig. 4. Distribution of errors (a) together with the approximate solution (dots) and the exact solution (solid line) (b) in time $t = 1$ ($N = M = 100$) (example 2)

Example 3. In this example, we assume the following data

$$\alpha = 1.7, \quad \lambda(x) = \frac{x}{100}, \quad c = 1000, \quad \varrho = 2100, \quad u^\infty = 100, \quad a = 0, \quad b = 1,$$

$$g(x, t) = -0.00334273 t^2 x^{0.3} + 4200000 t x,$$

$$h(t) = -\frac{0.01 t^2}{t^2 - 100}, \quad v(x) = 0, \quad q(t) = 0,$$

and the exact solution is of the form $u(x, t) = x t^2$.

Similarly like in the previous examples, we examine the size of the error in dependance on the grid density. Table 3 presents the errors for different grids. For 150×150 grid the maximal error is about $6.7 \cdot 10^{-3}$, while for 200×200 grid this error is equal to $5 \cdot 10^{-3}$.

Table 3

Maximal errors Δ_{\max} and average errors Δ_{avg} calculated for the respective grids (example 3)

Grid $N \times M$	Δ_{\max}	Δ_{avg}
10×10	$1.0000 \cdot 10^{-1}$	$2.5000 \cdot 10^{-2}$
50×50	$2.0000 \cdot 10^{-2}$	$5.0000 \cdot 10^{-3}$
70×70	$1.4286 \cdot 10^{-2}$	$3.5714 \cdot 10^{-3}$
100×100	$1.0000 \cdot 10^{-2}$	$2.5000 \cdot 10^{-3}$
150×150	$6.6667 \cdot 10^{-3}$	$1.6667 \cdot 10^{-3}$
200×200	$5.0000 \cdot 10^{-3}$	$1.2500 \cdot 10^{-3}$

5. Conclusions

In this paper the method of solving the one-dimensional heat conduction equation with the space fractional derivative and the mixed boundary conditions of the second and third kind is presented. For this purpose, the implicit finite difference method was used and $O(h^2)$ approximations for boundary conditions was applied. The described method approximates very well the exact solution, as we can see by analyzing the examples. With the increase of density grid, the errors of approximate solution decrease. The motivation for creating the algorithm for solving the investigated model with the boundary conditions of the second and third kind came from the expected possibility for using this approach also in solving the fractional inverse problem. Moreover, the authors intend in the future to consider the models with boundary conditions of fractional order.

References

1. Brociek R.: *Implicit finite difference method for time fractional heat equation with mixed boundary conditions*. Zesz. Nauk. PŚ., Mat. Stosow. **4** (2014), 73–87.
2. Carpinteri A., Mainardi F.: *Fractal and Fractional Calculus in Continuum Mechanics*. Springer, New York 1997.
3. Chen W., Ye L., Sun H.: *Fractional diffusion equations by the kansa method*. Comput. Math. Appl. **59** (2010), 1614–1620.
4. Diethelm K.: *The Analysis of Fractional Differential Equations*. Springer, Berlin 2010.
5. Feng L., Zhuang P., Liu F., Turner I., Yang Q.: *Second-order approximation for the space fractional diffusion equation with variable coefficient*. Progr. Fract. Differ. Appl. **1** (2015), 23–35.
6. Guo B., Pu X., Huang F.: *Fractional Partial Differential Equations and Their Numerical Solution*. World Scientific, Singapore 2015.
7. Klafter J., Lim S.C., Metzler R.: *Fractional dynamics. Recent advances*. World Scientific, New Jersey 2012.
8. Liu F., Zhuang P., Turner I., Burrage K., Anh V.: *A new fractional finite volume method for solving the fractional diffusion equation*. Appl. Math. Modelling **38** (2014), 3871–3878.

9. Meerschaert M.M., Benson D.A., Scheffler H.P., Becker-Kern P.: *Governing equations and solutions of anomalous random walk limits*. Phys. Rev. E **66** (2002), 102R–105R.
10. Meerschaert M.M., Scheffler H.P., Tadjeran Ch.: *Finite difference methods for two-dimensional fractional dispersion equation*. J. Comput. Phys. **211** (2006), 249–261.
11. Meerschaert M.M., Tadjeran Ch.: *Finite difference approximations for fractional advection-dispersion flow equations*. J. Comput. Appl. Math. **172** (2006), 65–77.
12. Meerschaert M.M., Tadjeran Ch.: *Finite difference approximations for two-sided space-fractional partial differential equations*. Appl. Numer. Math. **56** (2006), 80–90.
13. Metzler R., Klafter J.: *The restaurant at the end of the random walk: recent developments in the description of anomalous transport by fractional dynamics*. J. Phys. Rev. A **37** (2004), R161–R208.
14. Miller K., Ross B.: *An Introduction to the Fractional Calculus and Fractional Differential*. Wiley, New York 1993.
15. Mitkowski W., Kacprzyk J., Baranowski J.: *Advances in the Theory and Applications of Non-integer Order Systems*, Springer Inter. Publ., Cham 2013.
16. Murio D.A.: *Implicit finite difference approximation for time fractional diffusion equations*. Comput. Math. Appl. **56** (2008), 1138–1145.
17. Podlubny I.: *Fractional Differential Equations*. Academic Press, San Diego 1999.
18. Rabsztyń Sz., Słota D., Wituła R.: *Functions gamma and beta*, vol. 1 and 2. Wyd. Pol. Śl., Gliwice 2012 (in Polish).
19. Sabatier J., Agrawal O.P., Tenreiro Machado J.A.: *Advances in Fractional Calculus. Theoretical Developments and Applications in Physics and Engineering*. Springer, Dordrecht 2007.
20. Sudha Priya G., Prakash P., Nieto J.J., Kayar Z.: *Higher-order numerical scheme for the fractional heat equation with Dirichlet and Neumann boundary conditions*. Numer. Heat Transfer B **63** (2013), 540–559.
21. Sweilam N.H., Nagy A.M., El-Sayed A.A.: *On the numerical solution of space fractional order diffusion equation via shifted Chebyshev polynomials of the third kind*. J. of King Saud University – Science **28** (2016), 41–47.
22. Tadjeran Ch., Meerschaert M.M., Scheffler H.P.: *A second-order accurate numerical approximation for the fractional diffusion equation*. J. Comput. Phys. **213** (2006), 205–213.